

Analysis and prediction of ultimate strength of high-strength SFRC plates under in-plane and transverse loads

Ramadoss Perumal* and S. Palanivel

Department of Civil Engineering, Pondicherry Engineering College, Puducherry- 605014, India

(Received July 14, 2014, Revised November 18, 2014, Accepted November 22, 2014)

Abstract. Plates are most widely used in the hulls of floating concrete structures, bridge decks, walls of off-shore structures and liquid storage tanks. A method of analysis is presented for the determination of load-deflection response and ultimate strength of high-strength steel fiber reinforced concrete (HSSFRC) plates simply supported on all four edges and subjected to combined action of external compressive in-plane and transverse loads. The behavior of HSSFRC plate specimens subjected to combined uniaxial in-plane and transverse loads was investigated. The proposed analytical method is compared to the physical test results, and shows good agreement. To predict the constitutive behavior of HSSFRC in compression, a non-dimensional characteristic equation was proposed and found to give reasonable accuracy.

Keywords: steel fiber reinforced concrete plate; out-of-plane central deflection; load-deflection response; analytical model; ultimate strength prediction

1. Introduction

Concrete plates are used as structural elements in the hulls of floating concrete structures, floating bridges, walls of off-shore structures and liquid storage tanks. These plate elements are subjected to combined compressive in-plane loads due to the longitudinal bending of structure and transverse loads caused by hydrostatic pressure or deck loads. These plates resist loads in two way action and develop biaxial curvatures. A few analytical models exist and test results are available only for reinforced concrete plates under combined in-plane and transverse loads (Aghayere and MacGregor 1990a, b, Ghoneim and MacGregor 1994a, b). Bao *et al.* (1997), Malekzadeh (2007) have given an analytical solution for the bending and buckling of orthotropic steel plates and composite thin plates, respectively. Oiao *et al.* (2013) have studied on ultimate strength predictions of simply supported square plates of laminated composite materials subjected to uniaxial in-plane compressive load. An analytical study for bending analysis of soft-core composite sandwich plates using improved high-order theory was carried out by Kheirikhah *et al.* (2012). A rigorous evaluation procedure for the cracked moment in RC beams and slabs arrived and suggested by Lopes and Lopes (2012). A numerical study with two constitutive models was carried out to estimate the flexural behavior of full-scale FRC slabs of different dimensions (Blanco *et al.* 2014).

A method of analysis is developed here based on the assumed deflection method. In this way

*Corresponding author, Associate Professor, E-mail: dosspr@gmail.com

calculation of the strength of a plate is reduced to one degree of freedom problem. A simple analytical model of the plate response based on a Fourier expansion of the deflection and lateral load is presented. The behavior of the high-strength steel fiber reinforced concrete plates, taking into account the non-linear material response using moment-curvature relationship, is determined by applying the theory of elasticity. Due to the non-linear nature of the stress-strain relations, use of numerical procedures rather than closed form solutions has been employed. The geometrical non-linearity is incorporated in the governing differential equation. An experimental program was already carried out to investigate the behavior of high-strength SFRC plates subjected to in-plane and transverse loads, with aspect ratio (L_y/L_x) or (a/b) of all the plates as 1 and length to thick ratio maintained as 20 (Ramadoss and Nagamani 2009). The results from the analysis are compared to the test results from an experimental study carried out by Ramadoss and Nagamani (2009). Good agreement was obtained for simply supported square plates containing varying fiber volume fraction.

2. Research significance

Most of the research carried out on metal and RC plates supported on four edges and subjected to combined loads or in-plane loads. A very few analytical methods are available to treat the situation of combined in-plane and transverse loads. The analytical methods for predicting the ultimate strength of steel fiber reinforced concrete plates (composite plates) subjected to combined in-plane and transverse loads have been scarce to the author's knowledge. This paper presents a simple analytical model for the prediction of ultimate strength of high-strength SFRC plates in a reasonably accurate manner. To predict the constitutive behavior of HSSFRC in compression, a non-dimensional characteristic equation was proposed.

3. Material constitute law

3.1 Constitutive model for stress-strain curve of SFRC in compression

Under pure flexure, the strength of plain concrete does not have a significant influence on the flexural capacity, but the steel fiber reinforced concrete (SFRC) has a significant effect on the flexural capacity compared to plain concrete. Under combined flexural and axial compression, strength of SFRC plays an important role in the determination of the section capacity, particularly, if the level of the in-plane load is significant. Compressive strength test was performed according to ASTM C 39-1992 standards using 150 mm dia. cylinder specimens, and flexural strength (modulus of rupture) test was conducted as per the specification of ASTM C 78-1994. Mechanical properties of the high-strength SFRC (HSSFRC) with varying fiber volume fraction ($V_f=0-1.5\%$) are given in Table 1.

The stress-strain behavior of HSSFRC with 150Ø cylinder compressive strength ranging from 52 to 70 MPa has been investigated. Elastic modulus (secant modulus), $E_{cf} = 29.68-36.79$ GPa and Poisson's ratio, $\nu = 0.19-0.25$ obtained for HSSFRCs are used in this analytical study. ACI Committee 318-1995 (2004) permits the use of any concrete stress-strain relationship that predicts section strength in substantial agreement with the results of compressive strength tests. Stress-

Table 1 Summary of experimental program and test results of HSSFRC

Plate Specimen	Specimen size (mm)	SF (%)	V_f (%)	f_{cf}^* (MPa)	f_{rf} (MPa)	Nx/f_{cf}^*h	q (kN/m ²)
A1	600×600×30	10	0	52.56	6.21	0.063	79.17
A2	600×600×30	10	1.0	56.01	7.73	0.060	125.27
A3	600×600×30	10	1.5	57.42	8.19	0	93.06
B1	600×600×30	15	0	55.7	6.84	0.060	106.11
B2	600×600×30	15	1	60.21	8.64	0.055	129.44
B3	600×600×30	15	1.5	61.17	9.28	0	95.83
C1	600×600×30	10	0	63.86	7.4	0.052	115.28
C2	600×600×30	10	1.0	68.91	9.32	0.048	133.33
C3	600×600×30	10	1.5	69.67	10.13	0	99.44
D1	600×600×30	15	0	64.28	8.16	0	65.83
D2	600×600×30	15	1.0	69.74	10.32	0.048	142.78
D3	600×600×30	15	1.5	70.32	11.08	0.047	159.86

Note: $L_x = L_y = 600$ mm; $h =$ thickness of plate = 30 mm; aspect ratio = $L_y/L_x = 1$; slenderness ratio (L_x/h) = 20; $Nx =$ in-plane load per unit width; $q =$ transverse load per unit area; SF (%) = silica fume replacement in percent; $V_f =$ steel fiber volume fraction.

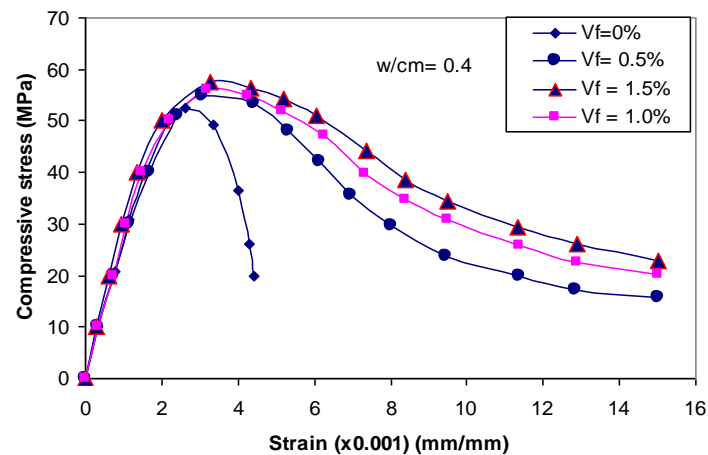


Fig. 1 Stress-strain curves for silica fume concrete and steel fiber reinforced concrete ($w/cm = 0.40$, SF content = 10%)

strain curves for HSC with 10% SF replacement (silica fume concrete) and steel fiber (crimped type) reinforced concrete, obtained using cylinder specimens are shown in Fig 1. From the stress-strain ($\sigma-\epsilon$) curves generated in this study (refer Fig. 1), it is seen that the post-peak segment of the curve is altered by the addition of steel fibers, and can also be observed that an increase in concrete strength increases the extent of curved portion in ascending branch and renders the drop in the descending part steeper for HSC and gradually flatter for SFRC. This gradual drop in the post peak region for SFRC is occurred because of matrix-fiber bond effect and three dimensional mechanism of crimped steel fibers. Although the drop in the post peak region is gradual for SFRC, there is a residual stress even at a strain as high as 0.015.

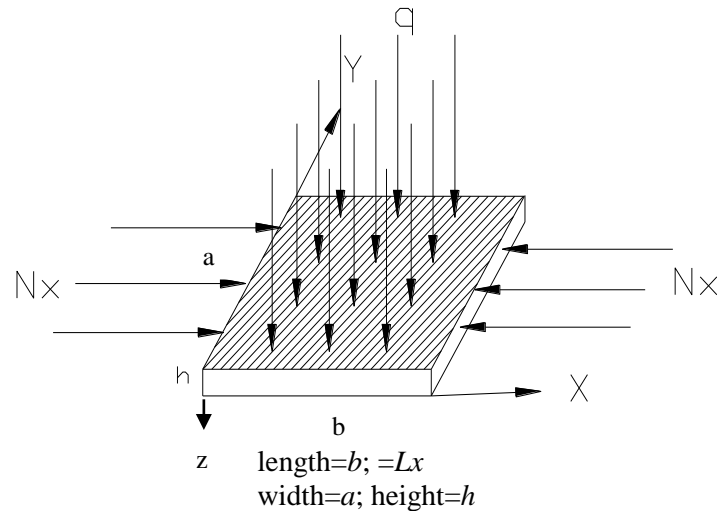


Fig. 2 Plate dimension, coordinate axes, and loading considered in testing (boundary condition: plate simply supported along four edges)

In an earlier study (Wee *et al.* 1996), a number of available models for plain concrete had been assessed, and a modified Carreira and Chu (1985) equation was found to be simple; provided a good correlation with the test results on HSC. The same model has been chosen here for high-strength steel fiber reinforced concrete. An analysis of test data generated in this study reveals that the model can adequately describe the ascending branch of the curve provided appropriate values of E_{it} , f_o , ε_o and β are used. A modified equation considering the material parameter to assess the concrete stress (f) at any given concrete strain (ε) is given as

$$\frac{f}{f_o} = \left[\frac{\beta(\varepsilon / \varepsilon_o)}{\beta - 1 + (\varepsilon / \varepsilon_o)^\beta} \right] \quad (1)$$

where

$$\beta = \frac{1}{1 - \frac{f_o}{\varepsilon_o E_{it}}} \quad (2)$$

where f_o = peak stress; ε_o = strain corresponding to peak stress; E_{it} = initial tangent modulus; f = stress corresponding to strain ε ; and β = material parameter that depends on the shape of the stress-strain curve, which is greater than or equal to 1.

The predictions using this proposed analytical model (Eq. (1)) were thus computed and compared with the experimental values, are in good agreement with the experimental curves. This type of work was carried out elsewhere by Ramadoss and Nagamani (2013). Thus, the proposed model (Eq. (1)) can be used to obtain the complete stress-strain (σ - ε) behavior of HSSFRC.

3.2 Load-deflection response

The test program was divided into four series of plates simply supported along four edges as

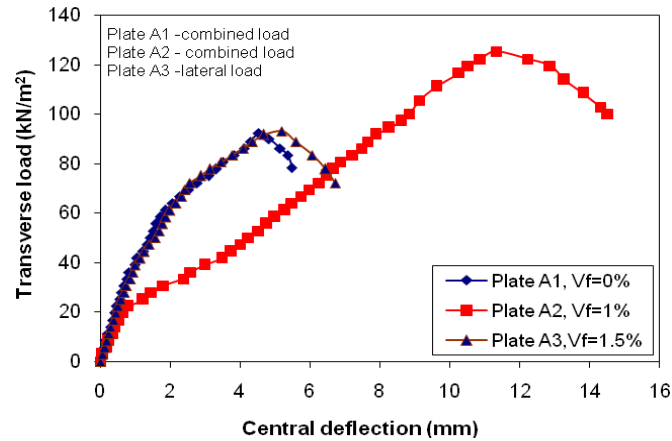


Fig. 3 Lateral load verses Out-of-plane center deflection for plate specimens A1, A2, and A3.

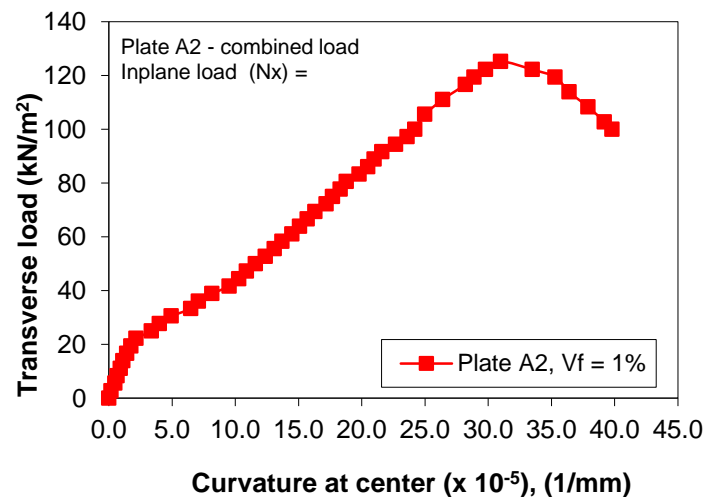


Fig. 4 Transverse load-Curvature diagram for a typical SFRC section (plate A2); in-plane load (N_x) = 100 kN/m

given in Table 1. The geometry of the typical rectangular plate element and loading considered in this experimental study is shown in Fig. 2. Table 1 gives the ratio of the applied in-plane load per unit width to the uniaxial strength of concrete multiplied by the plate thickness for all of the specimens. Fig. 3 shows the transverse load verses out-of-plane deflection ($P-\Delta$) at the center of the plate specimens (A1, A2, and A3). The SFRC specimens exhibited essentially a linear $P-\Delta$ response well beyond the load while the flexural cracks were first observed during the test. Each diagram is essentially a straight line up to the start of cracking. Beyond cracking, a rapid change of slope in the load- deflection curve was observed. On further loading, yielding of fibers started in one or more regions and spread through the areas still elastic. This continued till the yield line mechanism developed. A small out-of-plane deflection occurred in several specimens during the application of the in-plane loads. This deflection ranged from 0-2 % of the transverse load. The

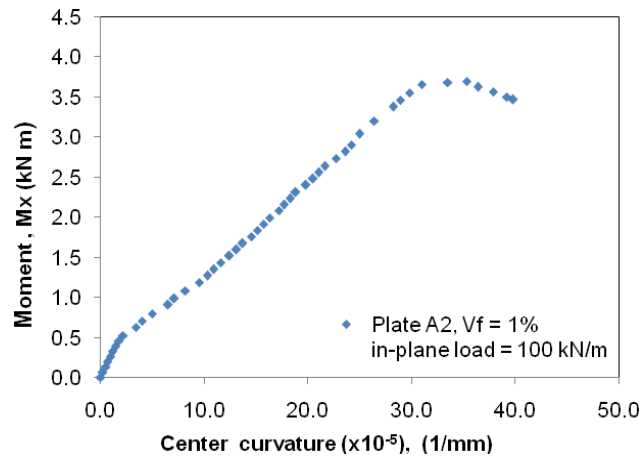


Fig. 5 Moment-Curvature diagram for a typical SFRC section (plate A2); in-plane load (N_x)=100 kN/m

level of the in-plane load ($N_x/f'_c h$) for all the specimens was moderate, in the sense that there is no possibility of collapse under in-plane load alone.

3.3 Moment–curvature relation

The non-linear behavior of a concrete member is characterized by the load-moment-curvature relationships of its cross section. The analytical method developed to calculate the $M-\theta$ relationship are based on application of the basic principles of equilibrium of forces and strain compatibility, assuming linear distribution of strain over cross section and using idealized stress-strain relations to represent the behavior of SFRC. Due to the non-linear nature of this stress-strain ($\sigma-\epsilon$) relation, use of numerical procedures rather than closed form solutions has been employed. Transverse (lateral) load Vs Center curvature for a high-strength SFRC plate section with in-plane load (N_x) = 100 kN/m is shown in Fig. 4. Moment-curvature diagram for a typical SFRC section with in-plane load (N_x) = 100 kN/m is shown in Fig. 5.

4. Analytical model for SFRC plate subjected to combined in-plane and transverse loads

4.1 Theoretical background

Several past attempts have been made to apply the methods of limit analysis to plates subjected to externally applied transverse loads and internally induced in-plane loads due to the support conditions or externally applied in-plane and lateral loads. To determine the ultimate transverse load using the limit analysis, the value of central deflection at the ultimate load must be known.

Equations for orthotropic plates derived in test books on ‘Theory of plates’ (Timoshenko and Woinowsky-Krieger 1959) and ‘Stability of structures’ (Bazant and Cedolin 1991), are needed for use in the proposed analytical model. A typical rectangular plate of length L_x , width L_y , and

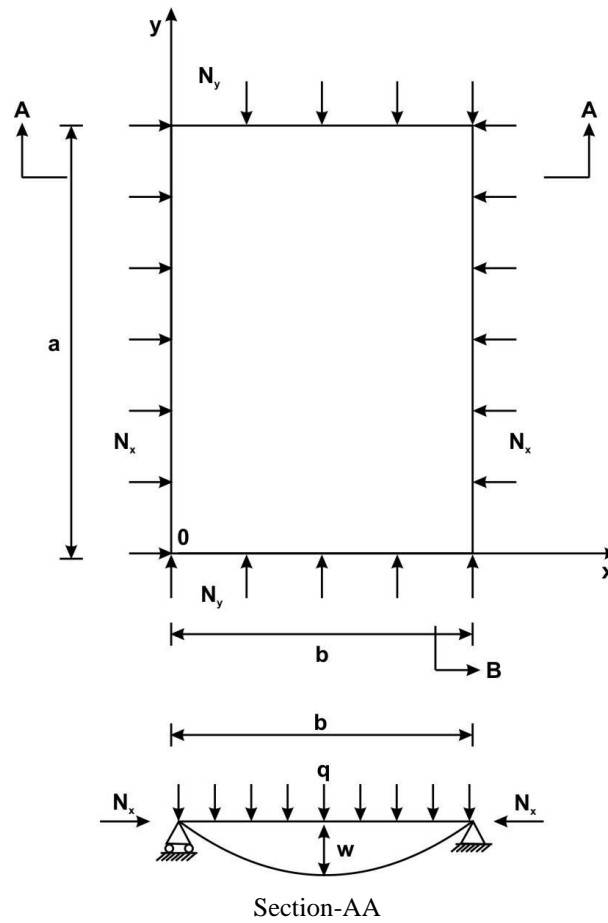


Fig. 6 Plate dimensions, coordinate axes, boundary condition and loading condition for analysis

uniform thickness h with a section along x - axis, as considered in the analysis is shown in Fig. 6. The x -, y -, and z - axes are longitudinal, transverse, and vertical axes, respectively. The uniform in-plane load per unit length, N_x and N_y are applied in the x and y directions to the sides $L_y (=a)$ and $L_x (=b)$, respectively. Both in-plane loads are applied on the thickness of the plates. In addition, there is a uniform lateral pressure (q) at any point (x,y) . The out-of-plane displacement from the flat surface is represented by ‘ w ’.

4.2 Analytical model

Based on the Kirchoff theory, the relationship between moments and deformations for elastic orthotropic plates are given as

$$M_x = -D_x (\partial^2 w / \partial x^2 + \nu_y \partial^2 w / \partial y^2) \tag{3}$$

$$M_y = -D_y (\partial^2 w / \partial y^2 + \nu_x \partial^2 w / \partial x^2) \tag{4}$$

$$M_{xy} = 2D_t (\partial^2 w / \partial x \partial y) \tag{5}$$

where

$$2D_t = (1 - \nu_x \nu_y) (\sqrt{D_x D_y}) \quad (6)$$

represents torsional rigidity of the plate, while D_x and D_y are the flexural rigidity in x - and y -directions, respectively. M_x and M_y are moments per unit width. M_x is about the y -axis and M_y is about the x -axis.

The equilibrium equation for an elastic orthographic plate under combined transverse load $q(x,y)$ per unit area and compressive in plane loads N_x and N_y per unit width in the x - and y -directions, respectively is given as

$$\partial^2 M_x / \partial x^2 - 2 \partial^2 M_{xy} / \partial x \partial y + \partial^2 M_y / \partial y^2 - N_x \partial^2 w / \partial x^2 - N_y \partial^2 w / \partial y^2 = -q(x,y) \quad (7)$$

The preceding equation is independent of the material properties and hence is valid for both elastic and plastic cases. Substituting the Eqs. (3) through (7), the governing differential equation for the deflection of the elastic orthotropic plate is written as

$$D_x \partial^4 w / \partial x^4 + 2H \partial^4 w / \partial x^2 \partial y^2 + D_y \partial^4 w / \partial y^4 = q(x,y) - N_x \partial^2 w / \partial x^2 - N_y \partial^2 w / \partial y^2 \quad (8)$$

where

$$H = 0.5 (\nu_x D_y + \nu_y D_x + 4D_t) \quad (9)$$

is called the "effective torsional rigidity" of the plate, while ν_x and ν_y are the Poisson's ratios in the x and y directions, respectively.

The equations derived are based on the following assumptions:

1. Small transverse deflections are assumed. This means membrane action is neglected.
2. Plane sections remain plane after bending. This implies that vertical shear strains are negligible.
3. The stress normal to the mid plane, σ_z is very small compared with other stress components and may be neglected.
4. The plate is initially flat.
5. The material is elastic and orthotropic.

There is an experimental evidence to suggest the effective Poisson's ratio to be zero, which is reasonable for a cracked concrete plate. For Poisson's ratio equal to zero, the Eqs. (6) and (9) reduce to the expressions given below for the concrete slab can be adopted.

$$2D_t = \sqrt{D_x D_y}; \quad H = 2D_t$$

Based on the preceding approximations, the differential equation of the plate problem in hand can be written as

$$D_x \partial^4 w / \partial x^4 + 4D_t \partial^4 w / \partial x^2 \partial y^2 + D_y \partial^4 w / \partial y^4 = q(x,y) - N_x \partial^2 w / \partial x^2 - N_y \partial^2 w / \partial y^2 \quad (10)$$

The uniform lateral load is represented by the trigonometric series

$$q(x,y) = 16q / \pi^2 \sum_{m=1}^{\infty} \sum_{n=1}^{\infty} \frac{1}{mn} \sin m\pi x / L_x \sin n\pi y / L_y \quad (11)$$

A sinusoidal shape of the deflection curve has been used by Bazant *et al.* (1991) for the analysis of RC beam-columns. The deflection surface can be expressed in the form of the double

sine series (Eq. (12)) which satisfies the boundary conditions for the simply supported plate with in-plane restrictions.

$$w(x, y) = \sum_{m=1}^{\infty} \sum_{n=1}^{\infty} w_0 \sin m\pi x/L_x \sin n\pi y/L_y \tag{12}$$

where m and n are positive odd integers ($m = 1, 3, 5, \dots$ and $n = 1, 3, 5, \dots$)

w_0 is the maximum transverse deflection occurs at the center of the plate elements.

Eqs. (11) and (12) are usually expressed in infinite series form. Herein, however, only a finite series to provide some acceptable tolerance is considered. In this analysis, six terms ($\bar{m} = \bar{n} = 5$) are used. Substituting this series in Eq. (10), we find the following expression for the coefficient w_0 .

$$w_0 = \frac{16q}{\pi^2 mn D \left(1 - \frac{N_x m^2 \pi^2}{L_x^2 D} - \frac{N_y n^2 \pi^2}{L_y^2 D} \right)} \tag{13}$$

In which m and n are odd integers 1, 3, 5 and $w_0 = 0$ if m or n or both are even numbers. Hence, the deflection of the plate is

$$w(x, y) = \sum_{m=1}^{\infty} \sum_{n=1}^{\infty} w_0 \sin m\pi x/L_x \sin n\pi y/L_y \tag{14}$$

where

$$D = \frac{D_x m^4 \pi^4}{L_x^4} + \frac{2D_x D_y m^2 n^2 \pi^4}{L_x^2 L_y^2} + \frac{D_y n^4 \pi^4}{L_y^4} \tag{15}$$

For such plates the maximum bending moment occurs at $x = L_x/2$ and $y = L_y/2$, and torsional moment occurs at the corners of the plate. The maximum moments are

$$M_{x,m} = N_x w_0 + \alpha_x q L_x^2 + N_x e_x \tag{16}$$

$$M_{y,m} = N_y w_0 + \alpha_y q L_x^2 + N_y e_y \tag{17}$$

$$M_{xy,m} = \alpha_{xy} q L_x L_y \tag{18}$$

where α_x , α_y and α_{xy} are moment coefficients depend upon the aspect ratio (L_y/L_x) of plate. e_x and e_y are the eccentricity of in-plane loads in x and y planes, respectively.

The curvatures can be approximated by the second derivatives of the deflection function as

$$\phi_x = w_{,xx} = -\frac{\partial^2 w}{\partial x^2} \tag{19}$$

$$\phi_y = w_{,yy} = -\frac{\partial^2 w}{\partial y^2} \tag{20}$$

$$\varphi_{xy} = w_{,xy} = -\frac{\partial^2 w}{\partial x \partial y} \quad (21)$$

Assuming the poisson's ratio to be zero at ultimate state (cracked) for the most of the practical cases, Eqs. (3) through (6) and Eqs. (19) through (21) give the moment-curvature relationships as

$$M_{x,m} = D_x \varphi_{x0} \quad (22)$$

$$M_{y,m} = D_y \varphi_{y0} \quad (23)$$

$$M_{xy,m} = \sqrt{D_x D_y} \varphi_{xy0} \quad (24)$$

From the above Eqs. (22) to (24), we obtain

$$M_{xy,m} = \sqrt{M_{x,m} M_{y,m}} \quad (25)$$

Using Eq. (14) and Eq. (19) through (21), we obtain

$$\varphi_{x0} = w_0 \frac{\pi^2}{L_x^2} \quad (26)$$

$$\varphi_{y0} = w_0 \frac{\pi^2}{L_y^2} \quad (27)$$

$$\varphi_{xy0} = w_0 \frac{\pi^2}{L_y L_x} \quad (28)$$

where, $L_x=b$; $L_y=a$

Hence, the curvature in the x-direction, at the center of the plate, is related to the lateral load by the relation

$$\varphi_{x0} = \sum_{m=1}^{\bar{m}} \sum_{n=1}^{\bar{n}} \frac{16qm}{L_x^2 D n} \frac{\sin \frac{m\pi}{2} \sin \frac{n\pi}{2}}{\lambda} \quad (29)$$

where φ_{x0} is the curvature at the center of the plate in the x-direction. In the preceding equation, λ is given by

$$\lambda = \left(1 - \frac{N_x m^2 \pi^2}{L_x^2 D} - \frac{N_y n^2 \pi^2}{L_y^2 D}\right) \quad (30)$$

The ratio (R) between the curvatures at the plate center in the y- and x- directions is given by

$$R = \frac{\varphi_{y,\max}}{\varphi_{x,\max}} = \frac{L_x^2}{L_y^2} = \frac{b^2}{a^2} \quad (31)$$

Hence, the curvature at the center of the plate in the y-direction is given by

$$\varphi_{y0} = R \varphi_{x0} \quad (32)$$

$$\varphi_{x0} = \frac{a^2}{b^2} \varphi_{y0}; \varphi_{y0} = \frac{b^2}{a^2} \varphi_{x0}; \varphi_{xy0} = \frac{b}{a} \varphi_{x0}$$

From Eq. (16), the total transverse load versus curvature relation obtained is as given in Eq. (33).

$$q = \frac{1}{\alpha_x b^2} \left(M_{x,m} - \frac{N_x b^2 \varphi_{x0}}{\pi^2} - N_x e_x \right) \quad (33)$$

where, $\varphi_{x0} = w_0 \frac{\pi^2}{b^2}$ is the maximum curvature in the x- direction

The constants α_x and α_y depend upon the aspect ratio (a/b) of the plate element should be less than 2, are determined by the yield line theory.

The procedure for assessing the transverse load (q) at ultimate failure for a given set of in-plane loads N_x and N_y per unit width of the plate is as follows:

1. Obtain the M - N - φ relationships for sections of unit width at the centre of the plate.
2. Assume a value of φ_{x0} or φ_{y0} and from the equation calculate the other value of curvature.
3. From the M - N - φ relationships derived in step 1, obtain M_{x0} and M_{y0} corresponding to φ_{x0} and φ_{y0} , respectively.
4. Compute the transverse load (q) for a given value of φ_{x0} and φ_{y0} .
5. Compute the center deflection (w) for a given value of φ_{x0} and φ_{y0} .
6. Increment φ_{x0} or φ_{y0} and repeat the steps 3 and 4.
7. Draw a plot of transverse load (q) Vs the curvature in the x- direction or y-direction/ or deflection (w). The peak of this curve is taken as ultimate transverse load (q).

5. Comparison of analytical predictions with test results

An analytical model is presented for predicting the central deflection of HSSFRC plates subjected to combined biaxial in-plane compressive and transverse (lateral) loads. The plates are assumed to be simply supported on four edges without in-plane restraints. The analytical model described was used to predict the ultimate strength of high-strength steel fiber reinforced concrete plates tested. Test results indicated that application of the in-plane load prior to transverse load or proportional loading lead to little difference in the load deflection response and ultimate strength. Plate specimens tested under transverse loads only cases, carried loads higher than those predicted by the yield-line analysis. Table 2 compares the maximum transverse load (ultimate strength) obtained from the test with the maximum load from proposed analytical model. Table 3 compares the maximum center deflection from the test with the deflection obtained from proposed analytical model using C++ program developed. The average test to predicted center deflection value ratio is 0.94, standard deviation is 0.14, and the coefficient of variation is 14.7 percent. The computation method is considered satisfactory in view of the nature of the problem being dealt with and the wide range of variables involved in the test program. It should be emphasized that the main purpose of the method described in the preceding is to obtain the maximum transverse load under controlled in-plane load. It is suitable for tracing the load-deflection behavior as long as the diagram for load-deflection is raised. Figs. 7 and 8 show comparisons between the analytical and

Table 2 Comparison of transverse load from test with the ultimate prediction from model

Plate Specimen	Maximum transverse load from test (kN/m ²)	Maximum transverse load from analysis (kN/m ²)	Test/ predicted	Test/ predicted (yield) capacity
A1	79.17	7.28	0.64	-
A2	125.27	9.49	1.19	-
A3	93.06	6.76	0.77	1.527
B1	106.11	8.04	0.77	-
B2	129.44	9.25	1.16	-
B3	95.83	6.68	0.76	1.388
C1	115.28	7.9	0.67	-
C2	133.33	8.53	1.20	-
C3	99.44	6.29	0.78	1.345
D1	65.83	4.42	0.80	1.105
D2	142.78	9.13	1.11	-
D3	159.86	10.15	1.02	-
Mean:			0.900	
Coefficient of variation (%):			24.277	
Standard deviation:			0.218	

Table 3 Comparison of center deflection from test with the predicted value from model

Plate Specimen	Maximum center deflection from test (kN/m ²)	Predicted deflection from analysis (kN/m ²)	Test / predicted
A1	4.63	5.87	0.79
A2	11.32	9.89	1.14
A3	5.19	6.26	0.83
B1	5.72	7.04	0.81
B2	10.75	9.52	1.13
B3	5.1	6.12	0.84
C1	5.26	6.35	0.83
C2	10.23	8.93	1.15
C3	4.89	5.67	0.86
D1	3.52	4.22	0.83
D2	10.16	9.63	1.06
D3	10.35	10.15	1.02
Mean:			0.940
Coefficient of variation (%):			14.72
Standard deviation:			0.138

experimental load-deflection curves for high-strength SFRC plates with and without in-plane load containing fiber volume fractions, $V_f=1$ and 1.5%, respectively. In the ascending branch of the lateral load-deflection curves, the curves indicate a good agreement between the test and analysis. But, there is a deviation in the load-deflection curves near the ultimate load which is due to the formation of cracking along the yield lines in attaining the ultimate load. Although the analysis is presented for biaxial in-plane loads, it has been checked against uniaxially loaded plates. The analytical results are compared with experimental values; maximum loads are well predicted by

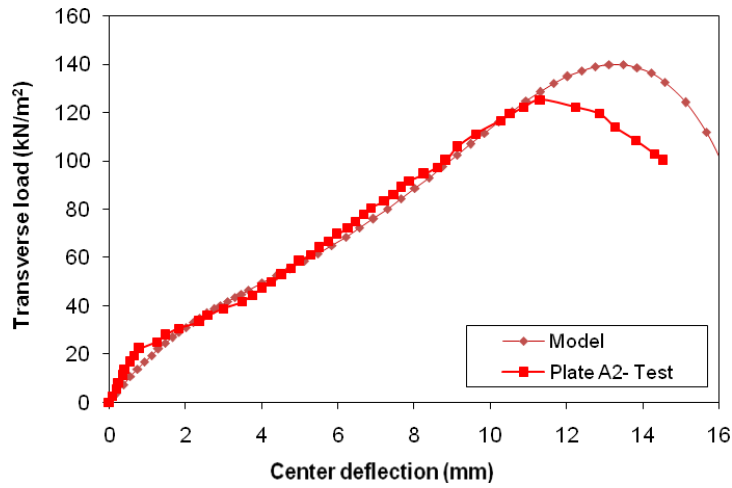


Fig. 7 Transverse load-deflection curve for plate specimen A2: Test verse analytical prediction

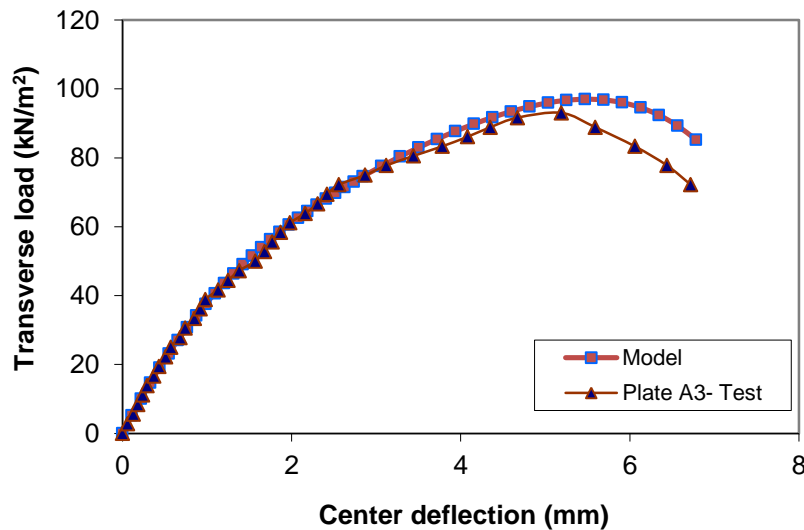


Fig. 8 Transverse load-deflection curve for plate specimen A3: Test verse analytical prediction

the analytical model, and reasonably good agreement is reached.

Central deflections of HSSFRC plate elements were also computed using ANSYS software considering the following parameters.

Material properties: Ultimate compressive stress (f'_{cf} or f_o); Modulus of rupture (f_{rf}); Modulus of elasticity (static modulus) (E_{cf}); Poisson's ratio (ν).

Plate parameters and boundary condition: Plate thickness (h); Aspect ratio (L_y / L_x); Slenderness ratio (L_y / h); All the edges are simply supported without in-plane restraints.

Computed central deflections of the plate elements were compared with the experimental values given in Table 2, and the absolute variation obtained is within 6%.

6. Summary and conclusions

Plate specimens were tested for combined loads, and transverse load only cases. Table 1 shows the properties of each specimen as well as the maximum transverse load per unit area, and the uniform in-plane load per unit width applied in the x-direction. The transverse load versus out-of-plane deflection relationship of specimen tested under in-plane and lateral loads is given in Fig. 3 to show the behavior of the HSSFRC plate element subjected to combined loads. Proportional loading or prior application of in-plane load resulted essentially in the same lateral load-deflection response and the same ultimate strength. The analytical method described in this paper is to obtain the ultimate transverse load under controlled in-plane load.

In this analytical study, the following conclusions are drawn:

1. Plate specimens tested under transverse loads only, carried loads higher than those predicted by the yield-line analysis (Table 2). This is partly attributed to the significantly increased flexural strength and improved fiber bond resistance of the fibrous concrete.

2. The prediction capability of the analytical model presented for ultimate strength capacity of HSSFRC plates subjected to combined in-plane and transverse loads is quite comparable to experimental results.

3. The comparison of test results of maximum transverse loads with the predictions by the analytical model checked for uniaxially loaded plates is presented. The analytical results are compared with test results, and reasonably good agreement is reached.

4. Analytical non-dimensional characteristic equation proposed can be used to predict the constitutive behavior of HSSFRC in compression, and good agreement has been achieved with experimental results

References

- ACI Committee 318 (2004), Building code requirements for structural concrete (ACI 318-1995) and commentary (ACI 318R-1995), *American Concrete Institute*, Detroit.
- Aghayere, A.O. and MacGregor, J.G. (1990b), "Analysis of concrete Plates under combined in-plane and transverse loads", *ACI Struct. J.*, **87**(5), 539-547.
- Aghayere, A.O. and MacGregor, J.G. (1990a), "Test of Reinforced concrete plates under in-plane and transverse loads", *ACI Struct. J.*, **87**(6), 615- 622.
- ASTM C 39-1992 (1992), Standard test method for compressive strength of fiber reinforced concrete, *Annual book of ASTM Standards*, American Society for Testing and Materials.
- ASTM C 78-1994 (1994), Standard test method for flexural strength of fiber reinforced concrete, *Annual Book of ASTM Standards*, American Society for Testing and Materials.
- Bao, G., Jiang, W. and Roberts, J.C. (1997), "Analytical and finite element solutions for bending and buckling of orthotropic plates", *Int. J. Solids Struct.*, **34**(14), 1797- 1832.
- Bazant, Z.P. and Cedolin, L. (1991), *Stability of Structures*, Oxford University Press, New York.
- Bazant, Z.P., Cedolin, L. and Tabbara, M.R. (1991), "New method of analysis for slender columns", *ACI Struct. J.*, **88**(4), 391-401.
- Blanco, A., CAvalaro, S., De la Fuente, A. *et al.* (2014), "Application of FRC constitutive models to modeling of slabs", *Mater. Struct.*, DOI 10.1617/s11527-014-0369-5.
- Carriera, D.J. and Chu, K.H. (1985), "Stress-strain relationship for plain concrete in compression", *ACI Mater. J.*, **82**(6), 797-804.
- Ghoneim, M.G. and MacGregor, J.G. (1994a), "Tests of reinforced concrete plates under combined inplane and lateral loads", *ACI Struct. J.*, **91**(1), 19-30.
- Ghoneim, M.G. and MacGregor, J.G. (1994b), "Behavior of reinforced concrete plates under combined

- inplane and lateral loads”, *ACI Struct. J.*, **91**(2), 188-197.
- Kheirikhah, M.M, Khalili, S.M.R. and Malekzadeh Fard, K. (2012), “Analytical solution for bending analysis of soft-core composite sandwich plates using improved higher-order theory”, *Struct. Eng. Mech.*, **44**(1), 5-34.
- Lopes, A.V. and Lopes, S.M.R. (2012), “Importance of a rigorous evaluation of the cracked moment in RC beams and slabs”, *Comput. Concrete*, **9**(4), 275-291.
- Malekzadeh, P. (2007), “A DQ nonlinear bending analysis of skew composite thin plates”, *Struct. Eng. Mech.*, **25**(2), 161-180.
- Ramadoss, P. and Nagamani, K. (2009), “Behavior of high-strength fiber reinforced concrete plates under inplane and transverse loads”, *Struct. Eng. Mech.*, **31**(4), 371-382.
- Ramadoss, P. and Nagamani, K. (2013), “Stress-strain behavior and toughness of high-performance steel fiber reinforced concrete in compression”, *Comput. Concrete*, **11**(2), 149-167.
- Timoshenko, S.P. and Woinowsky-Kriger, S. (1959), *Theory of plates and shells*, McGraw-Hill Book Co., New York.
- Wee, Y.H., Chin, M.S. and Mansur, M.A. (1996), “Stress-strain relationship of high strength concrete in compression”, ASCE, *J Mater. Civ. Eng.*, **8**(2), 70-76.
- Yang, O.J., Hayman, B. and Osnes, H. (2013), “Simplified buckling and ultimate strength analysis of composite plates in compression”, *Compos. B Eng.*, **54**, 343-352.

CC

Notations

- HSSFRC = High-strength steel fiber reinforced concrete
- q = Intensity of continuously distributed load, kN/m^2 .
- N_x = Normal force per unit length of section in x-direction, kN/m .
- L_x or b = Length of plate in x-direction.
- L_y or a = Length of plate in y-direction.
- h = Thickness of plate element, mm
- a/b = aspect ratio
- w = out-of-plane center deflection
- ν = Poisson's ratio
- f_o = peak stress
- ϵ = strain corresponding to stress
- ϵ_o = strain corresponding to peak stress
- E_{it} = initial tangent modulus
- β = material parameter
- f'_{cf} = Compressive strength of HSSFRC at 28 days, MPa.
- f_{rf} = Flexural tensile strength of HSSFRC at 28 days, MPa.
- E_{cf} = Static elastic (secant) modulus of HSFRC at 28 days, GPa
- M_x = moment per unit width about the y- axis
- M_y = moment per unit width about the x- axis
- M_{xy} = torsion moment per unit width about the xy- axes
- w_o = centre deflection of the plate element
- ϕ or ϕ = center curvature of plate
- α_x , α_y and α_{xy} = moment coefficients for M_x , M_y , and M_{xy} , respectively.